NANOOBJECTS & NANOSTRUCTURING

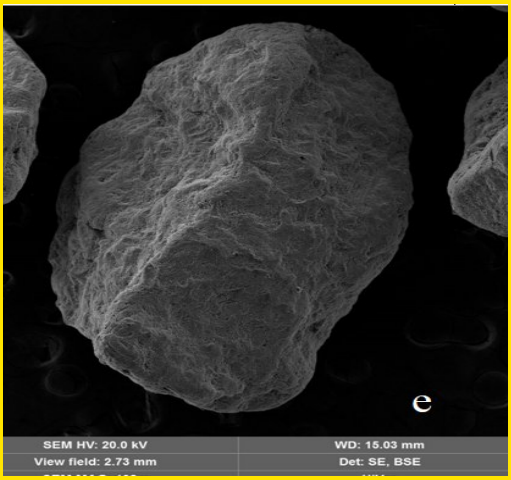

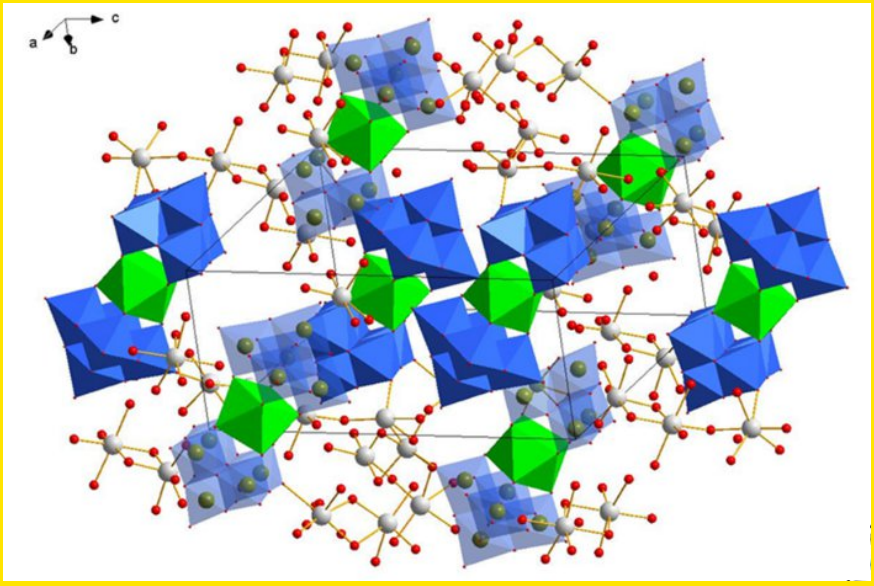

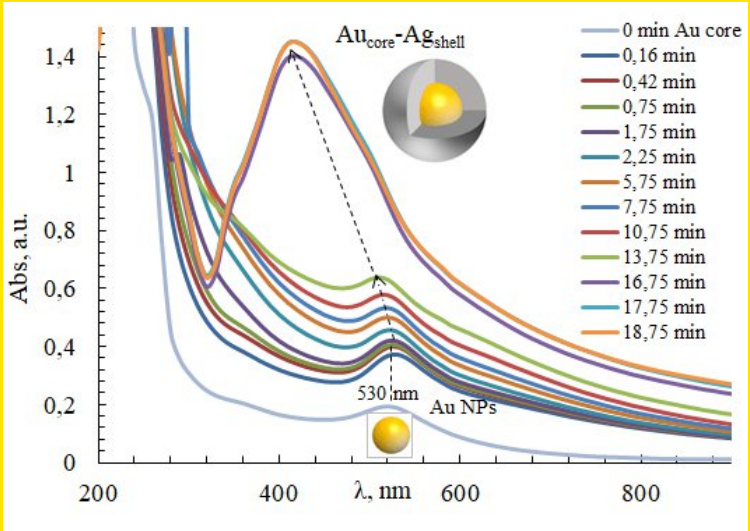

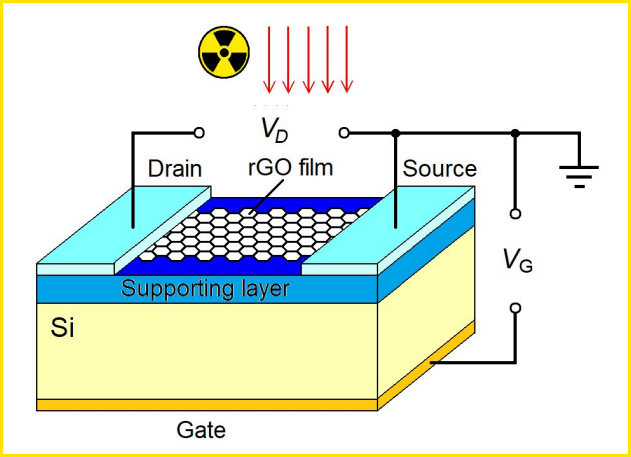

VOLUME II

NANOOBJECTS & NANOSTRUCTURING

COLLECTIVE MONOGRAPH

VOLUME II

NANOOBJECTS & NANOSTRUCTURING

COLLECTIVE MONOGRAPH

VOLUME II

Edited by
Lidiya M. Boichyshyn, D.Sc.
Oleksandr V. Reshetnyak, D.Sc.

Nova Printing Inc.
Mississauga, Ontario, Canada
2024

Nova Printing Inc.
2550 Goldenridge Road
Mississauga, ON, L4X 3S3
Tel: 905-281-3231

Nanoobjects & Nanostructuring. Volume II / Edited by Lidiya M. Boichyshyn and Oleksandr. V. Reshetnyak. – Mississauga, Ontario: Nova Printing Inc., 2024. - 210 + *xviii* p.

ISBN 978-1-7388295-1-4

ABOUT THE EDITORS

Lidiya M. Boichyshyn

Lidiya Boichyshyn, DSc, Professor, Professor of the Department of Physical and Colloid Chemistry of Ivan Franko National University of Lviv (Lviv, Ukraine), Chairwoman of Organizing Committee of the International Research and Practice Conference «Nanoobjects & Nanostructuring» (N&N). She is the author of four monographs, 22 patents and more than 450 publications in various journals and conference proceedings. His scientific activity is in the fields of physical chemistry of nanosystems, amorphous metallic alloys, power sources and chemical ecology. She is Deputy Editor-in-Chief of the scientific journal "*Proceedings of Shevchenko Scientific Society. Chemical Sciences*" (Lviv, Ukraine), Valid Member and Deputy Head of the Shevchenko Scientific Society (Lviv, Ukraine).

Oleksandr V. Reshetnyak

Oleksandr Reshetnyak, DSc, Professor, Laureate of the Borys Paton National Prize of Ukraine (2021), Head of the Department of Physical and Colloid Chemistry of Ivan Franko National University of Lviv (Lviv, Ukraine), Vice-chairman of Program Committee of the International Research and Practice Conference «Nanoobjects & Nanostructuring» (N&N). He is the author of five monographs and more than 500 publications in various journals and conference proceedings. His scientific activity is in the fields of physical chemistry of nanosystems, conductive polymers and its composites, electrochemistry of organic compounds. He is a Editor-in-Chief of the scientific journal "*Proceedings of Shevchenko Scientific Society. Chemical Sciences*" (Lviv, Ukraine) and Member of editorial boards of a collection of scientific works *«Visnyk Lvivskogo Universytetu, Seria Khimia»* (Lviv, Ukraine). He is also Valid Member of the Shevchenko Scientific Society (Lviv, Ukraine), member of the Bureau of the Scientific Council of the National Academy of Sciences of Ukraine on the problem of «Electrochemistry» (Kyiv, Ukraine).

Contact address:
6 Kyryla & Mefodiya Str., Lviv, 79005, Ukraine
Tel: (+38) (032) 260-03-97

E-mails:
lidiya.boichyshyn@lnu.edu.ua
oleksandr.reshetnyak@lnu.edu.ua

CONTENTS

Chapter 3

SYNTHESIS AND APPLICATION OF Eu(III)-CONTAINING HETEROPOLY SALTS WITH PEACOCK–WEAKLEY TYPE ANION

O. Yu. Mariichak, G. M. Rozantsev, S. V. Radio

Vasyl' Stus Donetsk National University, 21027 Vinnytsia, Ukraine

Corresponding author: radio@donnu.edu.ua

Contents

Abstract

The conditions for the formation of Eu(III)-containing heteropoly oxotungstate were established in an acidic solution with acidity $Z = \nu(H^+)/\nu(WO_4^{2-}) = 0.80$ in the Na_2WO_4 – – HNO_3 – $Eu(NO_3)_3$ – H_2O system. It was found that during precipitation with the addition of an organic solvent (2-propanone), crystallization of the normal salt $Na_9[Eu(W_5O_{18})_2]\times$ $\times 35H_2O$ with plate-like surface morphology occurs. Single crystal X-ray diffraction analysis of $Na_9[Eu(W_5O_{18})_2]\cdot 35H_2O$ provided fundamental data for the crystal structure: $a = 12.928$, $b = 13.064$, $c = 21.427$ Å, $\alpha = 101.04$, $\beta = 103.43$, $\gamma = 103.03^0$, $V = 3\ 313.8$ Å^3, $Z = 2$, triclinic, P–1 space group.

It has been demonstrated that the polyhedron of the heteroatom Eu(III) is a square antiprism formed by two tetradentate lacunary isopoly tungstate anions $[W_5O_{18}]^{6-}$. Infrared (FT–IR) and FT-Raman spectroscopy methods have established the characteristic vibration set for the heteropoly tungstate anion with the Peacock–Weakley type of structure. It has been shown that changes in the composition of the cationic sublattices and the presence of varying amounts of H_2O molecules in the structure do not affect the bond lengths and valence angles in the heteropoly anion $[Eu(W_5O_{18})_2]^{9-}$. UV-vis spectroscopy has confirmed that the formation of the $[Eu(W_5O_{18})_2]^{9-}$ heteropoly anion occurs immediately after the mixing of reactants in stoichiometric amounts within the temperature range of 10–60°C. Analysis of the practically relevant properties of $Na_9[Eu(W_5O_{18})_2]\cdot nH_2O$ shows that Eu(III)-containing polyoxotungstates with the Peacock–Weakley type of structure are promising for use as luminescent materials, for the development of new composite materials for OLEDs, and for use in analytical chemistry as detectors for H_2O_2, acidic, and basic gaseous compounds.

3.1 Introduction

Polyoxometalates (POMs) are a class of coordination compounds consisting of MO_6 polyhedra (M – 3d metal atoms from groups V–VI) connected by shared vertices, edges, or, though quite atypical and rare, faces. POMs attract significant interest due to their potential applications in various fields such as catalysis, magnetism, photochemistry, electrochemistry, and biological chemistry. The advancement of these fields relies on the synthesis of new POMs with unique properties. Over the past decades, research on lanthanide-containing POMs has been conducted, motivated by the study of the luminescent properties of such compounds and their ability to provide potential applications in materials science. The strategy of incorporating lanthanide ions into the structures of POM anions has been successfully applied in recent years, resulting in several promising complexes. Lanthanide-

containing POM derivatives find applications in diverse areas including the development of full-color displays, luminescent probes, catalysis, and medicine.

POMs represent a large class of inorganic solids. In many ways, POMs can be considered an ideal "nanomaterial" for biological applications such as imaging. They are monodispersed due to being inorganic crystals, have low cytotoxicity, and are sufficiently small (less than 5 nm) to be useful in cellular processes such as endocytosis. Most of them are water-soluble and can be functionalized with organic ligands, which is beneficial for further attachment to biomolecules. The diversity in POM structures and components gives rise to a significant number of potential biological tags. This variety is crucial for tuning excitation and emission wavelengths by selecting the appropriate building blocks of POMs and heteroatoms.

In this study, the aim was to establish optimal conditions for the synthesis and to synthesize crystalline sodium heteropoly decatungstoeuropate(III), determine its crystal structure, and perform a comparative analysis of the structure of the heteropoly anion with the Peacock–Weakley type in salts with varying content of crystallization H_2O molecules, different compositions of the cationic framework, and obtained through various procedures. The results are detailed in the following sections:

application of Eu(III)-containing heteropoly salts with Peacock–Weakley type anion;
determination of synthesis conditions for sodium heteropoly decatungstoeuropate(III) through self-assembly in an acidic aqueous solution of sodium tungstate;
use of FT–IR and FT–Raman spectroscopy for identifying the structure of the anion;
elucidation of the crystal structure of sodium heteropoly decatungstoeuropate(III), $Na_9[Eu(W_5O_{18})_2]\cdot nH_2O$;
results of comparing structural parameters (bond lengths and valence angles) in the heteropoly anion $[Eu(W_5O_{18})_2]^{9-}$ in salts with different cationic and hydration compositions.

3.2 Application of Eu(III)-Containing Heteropoly Salts with Peacock–Weakley Type Anion

Interest in studying Eu(III)-containing polyoxotungstates is primarily driven by the luminescent properties of these compounds, which are attributed to the energy transitions of inner f-electrons shielded from external influences by $5s^25p^6$ electrons [1]. Thus, in [2], a new photoluminescent layered nanocomposite film of an ionic complex formed by the Eu(III)-containing heteropoly anion $[Eu(W_5O_{18})_2]^{9-}$ and the hexadecyltrimethylammonium cation $C_{16}TA^+$ was obtained. The salt was obtained through supramolecular self-assembly of $Eu(NO_3)_3$ and Na_2WO_4 in an acidic aqueous solution using acetic acid, following the methodology proposed by Peacock and Weakley [3].

In [4], $Na_9[Eu(W_5O_{18})_2]\cdot 18H_2O$ (Eu-POM) was synthesized and a new method for detecting H_2O_2 (at ppm levels) based on fluorescence was developed by creating stabilized, thin, and transparent luminescent films composed of Eu-POM and environmentally friendly

chitosan (CS) (Figure 3.1). The prepared Eu-POM/CS films appear red under ultraviolet light (λ = 365 nm). Fluorescence spectroscopy was used to study the Eu-POM/CS films, and it was found that their fluorescence intensity is significantly higher than that of the solid Eu-POM salt (Figure 3.2).

The photoluminescent properties of the obtained Eu-POM/CS films were utilized to monitor H_2O_2 content, and it was found that as the H_2O_2 concentration increased from 0 to 88 μM, the fluorescence intensity of the thin films at 622 nm gradually decreased. It is noted that the degree of luminescence quenching in Eu-POM/CS is related to the H_2O_2 concentration. In other words, [4] demonstrates a new, simple method for detecting H_2O_2 at ppm levels using fluorescent films.

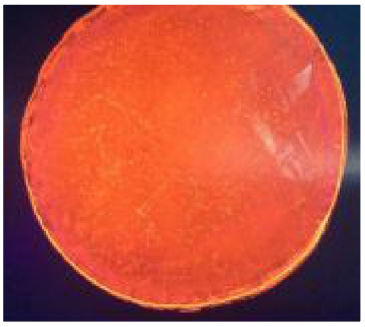

Figure 3.1 Eu-POM/CS film under UV irradiation (λ = 365 nm) (taken from [4])

Figure 3.2 (at the bottom) Fluorescence spectra: (*a*) solid Eu-POM and Eu-POM/CS film; (*b*) time-resolved fluorescence spectra for solid Eu-POM, Eu-POM solution, and Eu-POM/CS film (taken from [4])

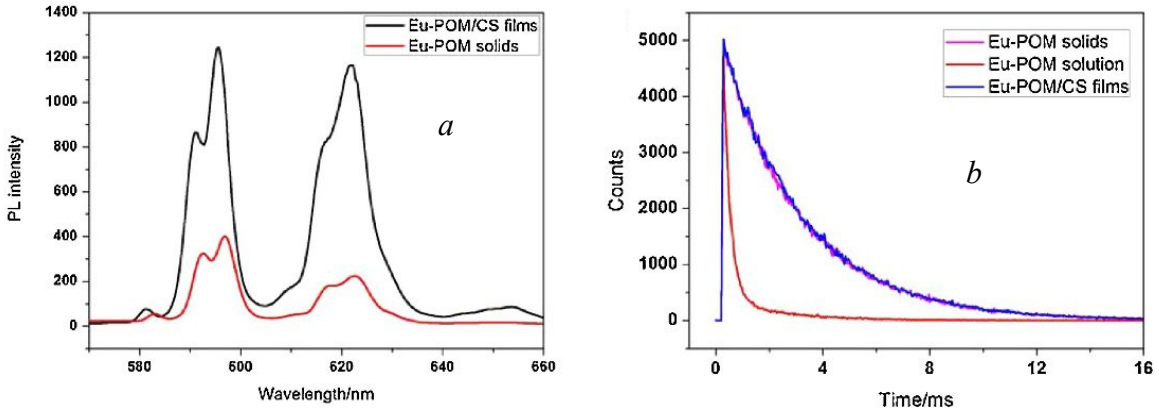

In [5], the crystalline salt $Na_9[Eu(W_5O_{18})_2]\cdot 32H_2O$ was synthesized using the procedure proposed by Peacock and Weakley [3], with $Na_2WO_4\cdot 2H_2O$, CH_3COOH (pH 7–7.5), and $Eu(NO_3)_3\cdot 6H_2O$ in solution at 80–90°C. The obtained salt was used to produce crystalline salts through an exchange reaction in a solution with a pH of 6.5 and Eu^{3+}, Sm^{3+}, and Tb^{3+} ions in the cationic sublattice, yielding $Eu_3[Eu(W_5O_{18})_2]\cdot 24H_2O$ (S1), $Sm_3[Eu(W_5O_{18})_2]\cdot 23H_2O$ (S2) та $Tb_3[Eu(W_5O_{18})_2]\cdot 25H_2O$ (S3). The isolated salts were characterized using powder X-ray diffraction analysis, FTIR spectroscopy, elemental analysis, and thermogravimetric analysis, confirming the presence of the $[Eu(W_5O_{18})_2]^{9-}$ anion in their structure and their isostructurality.

The photophysical properties, such as fluorescence spectra and fluorescence lifetimes, were also investigated. In addition to the characteristic Eu^{3+} emission ($^5D_0 \rightarrow {}^7F_{0,1,2,3,4}$)

observed in S1 and S2, compound S3 also exhibits the characteristic Tb^{3+} emission ($^5D_4 \rightarrow {}^7F_{6,4}$). The authors attribute this to different energy transfer mechanisms: S2 follows a resonant energy transfer mechanism from Sm^{3+} to Eu^{3+}, while S3 involves a cross-relaxation mechanism from Tb^{3+} to Eu^{3+}. Thus, the study [5] demonstrates that the luminescent mechanisms are dictated by the crystalline structure and composition, which in turn influence the luminescent properties. This is essential for designing and developing materials and devices with specific optical characteristics based on Ln(III)-containing polyoxotungstates.

In [6], efforts were focused on developing active luminescent sensors and switches based on $Na_9[Eu(W_5O_{18})_2]\cdot 32H_2O$ and agarose. Highly transparent, flexible thin films were obtained (Figure 3.3), which exhibit strong red emission from Eu(III) ions. The luminescence of these thin films is sensitive to acidic and basic gases – HCl gas quenches the luminescence, while NH_3 gas restores it. This not only suggests promising applications for these nanocomposite films in luminescent probes but also provides a simple method for implementing a luminescent switch using a two-component hybrid film system.

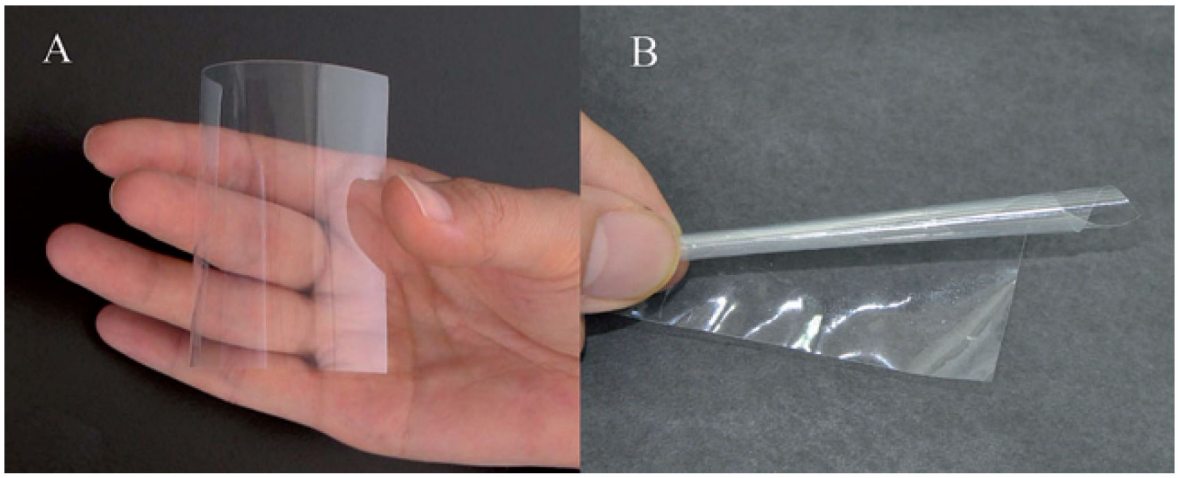

Figure 3.3 (A) Transparent flexible nanocomposite film based on $Na_9[Eu(W_5O_{18})_2]\cdot 32H_2O$ and agarose; (B) Nanocomposite film rolled into a tube (taken from [6])

In [7], thin monolayer films based on $Na_9[(Eu_mTb_nCe_{1-m-n})(W_5O_{18})_2]\cdot xH_2O$, which exhibit luminescent emission, were synthesized. The synthesis of yellowish crystals $Na_9[(Eu_{0,111}Tb_{0,222}Ce_{0,667})(W_5O_{18})_2]\cdot xH_2O$ (Ce : Tb : Eu = 3 : 1 : 0.5, compound 1), $Na_9[(Eu_{0,059}Tb_{0,235}Ce_{0,705})(W_5O_{18})_2]\cdot xH_2O$ (Ce : Tb : Eu = 3 : 1 : 0.25, compound 2), $Na_9[(Eu_{0,0244}Tb_{0,244}Ce_{0,732})(W_5O_{18})_2]\cdot xH_2O$ (Ce : Tb : Eu = 3 : 1 : 0.1, compound 3), $Na_9[(Eu_{0,0184}Tb_{0,245}Ce_{0,737})(W_5O_{18})_2]\cdot xH_2O$ (Ce : Tb : Eu = 3 : 1 : 0.075, compound 4), $Na_9[(Eu_{0,0123}Tb_{0,246}Ce_{0,741})(W_5O_{18})_2]\cdot xH_2O$ (Ce : Tb : Eu = 3 : 1 : 0.05, compound 5), $Na_9[(Eu_{0,04}Tb_{0,32}Ce_{0,64})(W_5O_{18})_2]\cdot xH_2O$ (Ce : Tb : Eu = 4 : 2 : 0.25, compound 6), and $Na_9[(Eu_{0,01}Tb_{0,200}Ce_{0,790})(W_5O_{18})_2]\cdot xH_2O$ (Ce : Tb : Eu = 4 : 1 : 0.05, compound 7) was carried out following the Peacock and Weakley procedure. The obtained films are characte-

rized by color luminescence across a wide range (blue, green, red, and white emission), achieved by adjusting the molar ratio of Ce^{3+} : Tb^{3+} : Eu^{3+} in the anion $[(Eu_mTb_nCe_{1-m-n})\times$ $\times(W_5O_{18})_2]^{9-}$, with statistically distributed lanthanides in the heteroatom position (Figure 3.4). Thin films were produced by applying a coating to a quartz glass substrate using the spin coating technique. It was demonstrated that the fluorescence intensity can be adjusted by varying the ratio of lanthanides in the initial solution. The films obtained in [7] were characterized by FTIR spectroscopy, X-ray fluorescence analysis, elemental analysis, UV spectroscopy, and SEM. The authors note that the thin films they produced are planar, homogeneous, with low surface roughness, and potentially suitable for designing optical functional materials based on polyoxometalates and for use in displays.

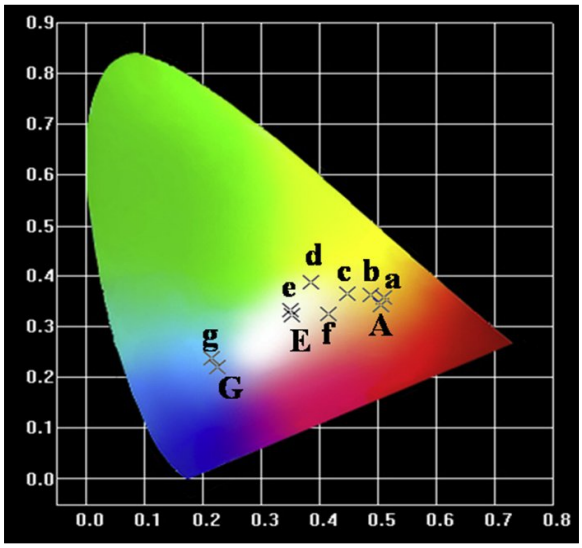

Figure 3.4 Color coordinates of compounds 1–7 and films based on compounds 1 (F1), 5 (F5), 7 (F7): a (0.511, 0.358) for 1; b (0.487, 0.363) for 2; c (0.415, 0.324) for 3; d (0.385, 0.388) for 4; e (0.349, 0.332) for 5; f (0.448, 0.365) for 6; g (0.216, 0.237) for 7; A (0.505, 0.342) for film F1; E (0.353, 0.323) for film F5; G (0.225, 0.220) for film F7 (taken from [7])

In [8], the interaction of $Na_9[Eu(W_5O_{18})_2]\cdot 32H_2O$ (EuW_{10}) with various amino acids was studied, leading to the spontaneous formation of vesicles (Figure 3.5). These vesicles showed enhanced luminescence for complexes of EuW_{10} with arginine (Arg), lysine (Lys), and histidine (His) while quenching of luminescence was observed in complexes of EuW_{10} with glutamic acid (Glu) or aspartic acid (Asp). The results obtained in [8] indicate that the luminescence of $[Eu(W_5O_{18})_2]^{9-}$ can be enhanced by adding alkaline amino acids (Arg, Lys, or His), while the addition of acidic amino acids (Glu, Asp) leads to quenching of the luminescence. And the addition of nonpolar amino acids (Leu, Ala, or Phe) does not affect the luminescent properties. Additionally, the hybrid material served as a fluorescence sensor with effective dopamine detection compared to other biomolecules. It was anticipated that these “amino acid–inorganic” hybrids would have significant applications in biosensors, bioanalytical devices, pharmaceutical applications, and industrial biocatalysis.

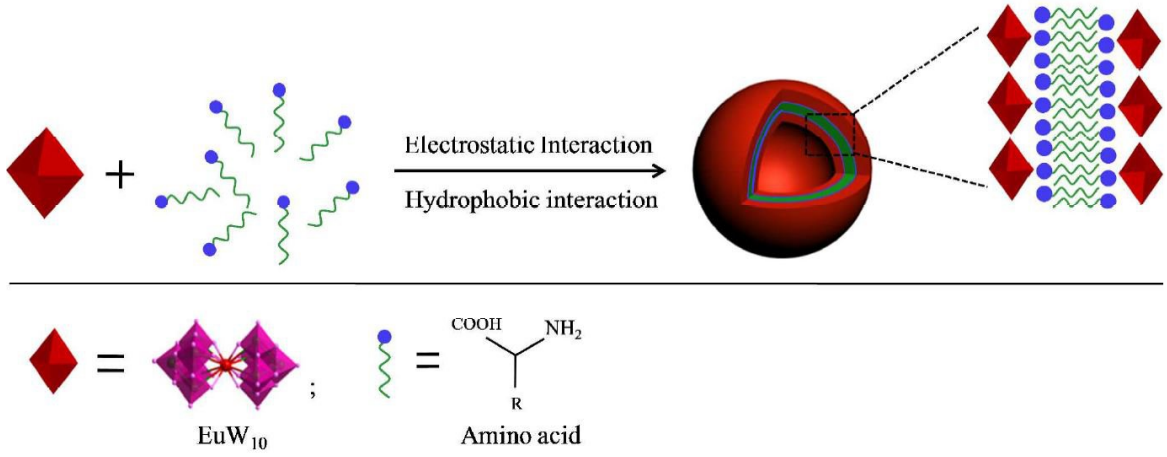

Figure 3.5 Scheme of preparation of vesicles based on $[Eu(W_5O_{18})_2]^{9-}$ and amino acids (taken from [8])

The results obtained in [8] indicate that the luminescence of $[Eu(W_5O_{18})_2]^{9-}$ can be enhanced by adding alkaline amino acids (Arg, Lys, or His), while the addition of acidic amino acids (Glu, Asp) leads to quenching of the luminescence. And the addition of non-polar amino acids (Leu, Ala, or Phe) does not affect the luminescent properties. Additionally, the hybrid material served as a fluorescence sensor with effective dopamine detection compared to other biomolecules. It was anticipated that these "amino acid–inorganic" hybrids would have significant applications in biosensors, bioanalytical devices, pharmaceutical applications, and industrial biocatalysis.

The review of scientific literature indicates that Eu(III)-containing heteropoly tungstates are promising for use as luminescent materials. These materials have potential applications in developing new combined materials for OLEDs and integrating multiple lanthanide ions into a single matrix can offer a wide color range for display screens. This necessitates high standards for the synthesis methods of the starting matrices, highlighting the relevance of this research. To address this, a study was conducted on the interaction in the aqueous solution of the $Eu(NO_3)_3 – Na_2WO_4 – HNO_3 – H_2O$ system at the acidity of $Z = \nu(H^+)/\nu(WO_4^{2-}) = 0.80$. A procedure was proposed for rapidly synthesizing a single-phase $Na_9[Eu(W_5O_{18})_2]\cdot 35H_2O$ sample with a plate-like surface morphology using a straightforward procedure in a short time.

3.3 Synthesis and Structural Characterization of $Na_9[Eu(W_5O_{18})_2]\cdot 35H_2O$

To investigate the formation of Eu(III)-containing heteropoly anion with a Peacock–Weakley type of structure via self-assembly in solution, UV-vis spectroscopy was used to analyze the processes occurring in the solution (Spekol 2000, Analytik-Jena). During the study of the formation of $[Eu(W_5O_{18})_2]^{9-}$ in the temperature range from 10 to 60ºC, changes in the UV-vis spectrum of the heteropoly anion were compared with changes

in the absorp-tion of an $Eu(NO_3)_3$ solution in the same temperature interval. In both experiments the Eu(III) concentration was consistent, totaling $1 \cdot 10^{-2}$ mol/L. Furthermore, the solution of $[Eu(W_5O_{18})_2]^{9-}$ was examined at 25℃ following a 24-hour heating period at 100℃ using a reflux condenser.

The research results indicated a hypochromic shift in the $[Eu(W_5O_{18})_2]^{9-}$ solution compared to Eu^{3+} (see Figure 6), observed at all temperatures immediately after the preparation of the respective solutions. Figure 3.6 shows two absorption maxima at 393.8 nm and 394.4 nm, corresponding to europium nitrate and the solution corresponding to the stoichiometry of the $[Eu(W_5O_{18})_2]^{9-}$ heteropoly anion. It can be observed that there is a direct proportional relationship between the absorption intensity and the temperature change: the absorption intensity decreases with decreasing temperature from 60 to 10°C for both $Eu(NO_3)_3$ (I) and the heteropoly anion (II), respectively.

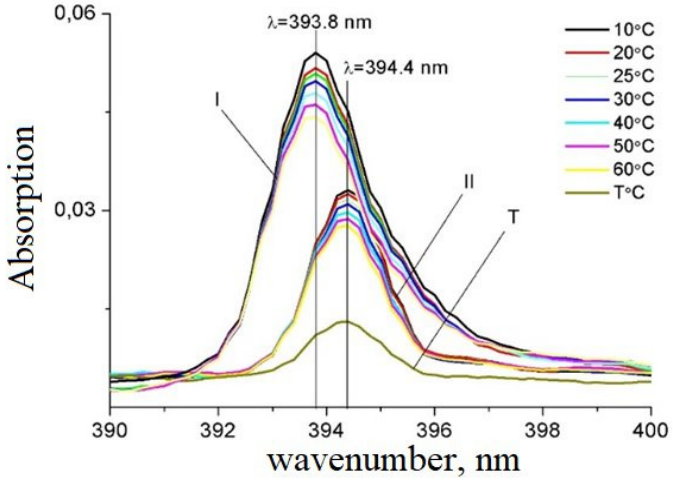

Figure 3.6. Absorption spectra: I – $Eu(NO_3)_3$ (C = 0.01 mol/L); II – $Na_9[Eu(W_5O_{18})_2] \cdot 35H_2O$ ($C(Eu^{3+})$ = 0.01 mol/L); T℃ – measurement at 25℃ after 24 hours of heating the $Na_9[Eu(W_5O18)_2] \cdot 35H_2O$ solution at 100℃

Thus, UV-Vis spectroscopy confirms that the heteropoly anion forms immediately upon mixing the reactants in stoichiometric amounts over the entire temperature range. This enables the synthesis to be conducted under standard laboratory conditions, whereas the synthesis procedure proposed by Peacock and Weakley [3] requires heating the solution to 90°C. This makes the procedure developed in this research more energy-efficient than the previously known one.

3.3.1 Synthesis and Chemical Analysis Methodology for the Salt

For the synthesis of the salt, a stoichiometric amount of $Eu(NO_3)_3$ was added with vigorous stirring to a 0.1 M solution of Na_2WO_4, acidified to acidity of $Z = \nu(HNO_3)$:

: $\nu(Na_2WO_4) = 0.80$ (where $\nu(HNO_3)$ and $\nu(Na_2WO_4)$ are the initial amounts of nitric acid and sodium tungstate, respectively). This value of Z, according to [9–11], corresponds to the formation of the heteropoly decatungstoeuropate(III) anion, $[Eu(W_5O_{18})_2]^{9-}$, in the solution:

$$Eu^{3+} + 10\ WO_4^{2-} + 8\ H^+ \rightleftharpoons [Eu(W_5O_{18})_2]^{9-} + 4\ H_2O.$$

The synthesis of $Na_9[Eu(W_5O_{18})_2]\cdot 35H_2O$ was conducted as follows. To 63.64 mL of distilled water, 19.44 mL of a sodium tungstate solution (C = 0.5144 mol/L) was added, and 9.37 mL of HNO_3 solution (C = 0.8535 mol/L) was added dropwise with vigorous stirring. Subsequently, 7.55 mL of $Eu(NO_3)_3$ solution (C = 0.1325 mol/L) was added dropwise with vigorous stirring. After obtaining the final solution, 100 mL of 2-propanone was added, and the solution was tightly sealed and left to stand for 3 days at 279 K with the formed precipitate. After this, the white plate-like precipitate was separated from the mother solution by filtration through a single "blue stripe" filter, washed with a cold mixture of distilled water and 2-propanone (v/v: 50:50), and dried in air to a constant mass. The resulting plate-like precipitate was then characterized using chemical analysis, FTIR and Raman spectroscopy.

Chemical analysis of the obtained white plate-like crystals was conducted using a methodology like that described in [9–11]. The chemical analysis results are as follows: calculated (mass %) for the colorless plate-like crystals of $Na_9[Eu(W_5O_{18})_2]\cdot 35H_2O$: Na_2O 8.2; Eu_2O_3 5.2; WO_3 68.1; H_2O 18.5; found (mass %): Na_2O 8.0; Eu_2O_3 5.0; WO_3 67.8; H_2O 18.4; yield 91%. The yield is quantitative; the loss is due to the dissolution of the crystalline precipitate on the filter during washing to remove counterions.

3.3.2 FTIR and Raman Spectroscopic Analysis of $Na_9[Eu(W_5O_{18})_2]\cdot 35H_2O$

Thus, colorless plate-like crystals of $Na_9[Eu(W_5O_{18})_2]\cdot 35H_2O$ were obtained from an aqueous solution of the system $Eu(NO_3)_3 – Na_2WO_4 – HNO_3 – H_2O$ with Z = 0.80, by adding 2-propanone (50 vol.%). The salt composition was determined by chemical analysis, and the assignment of the anion to the Peacock–Weakley structural type was made based on FTIR and Raman spectroscopy data. Specifically, the vibrational characteristics in the tungsten-oxygen framework in the FTIR and Raman spectra of the air-dried sample of the isolated salt (Figures 3.7 and 3.8) indicate the presence of a 10th row heteropoly anion with the Peacock–Weakley type of structure, $[Eu(W_5O_{18})_2]^{9-}$.

The set of vibrational modes in the FTIR spectrum of the isolated salt $Na_9[Eu(W_5O_{18})_2]\cdot 35H_2O$ (Figure 3.7) is characteristic of the site group of the heteropoly anion $[Ln(W_5O_{18})_2]^{9-}$ (Ln = La–Lu) and is identical to the FTIR spectra of salts whose crystal structures have been reliably determined by single-crystal X-ray diffraction analysis for salts with other Ln(III) heteroatoms [10–11].

The identification of the Raman spectrum of $Na_9[Eu(W_5O_{18})_2]\cdot 35H_2O$ (Figure 3.8) was carried out by comparing it with the results described in [12–13]. Intense peaks in the range of 930–980 cm^{-1} were attributed to vibrations of the bonds between tungsten atoms

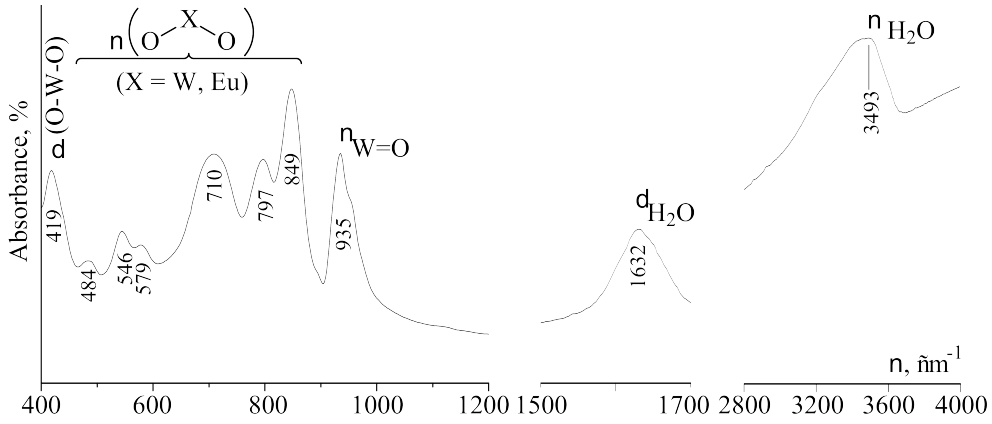

Figure 3.7 FT-IR spectrum for $Na_9[Eu(W_5O_{18})_2]\cdot 35H_2O$ (in KBr, Spectrum BXII FTIR Spectrometer, Perkin Elmer)

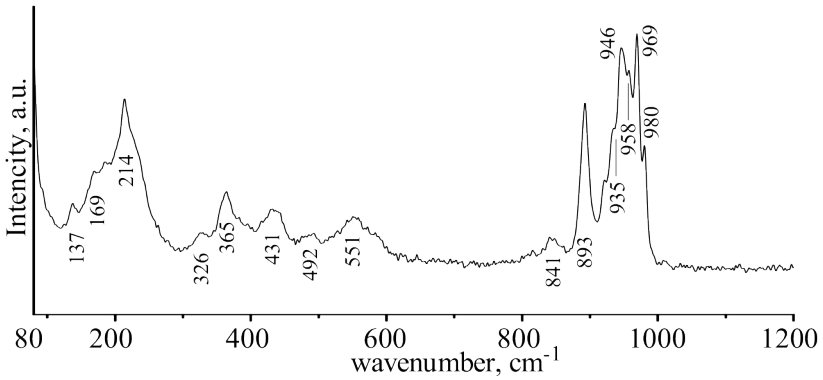

Figure 3.8 Raman spectrum for $Na_9[Eu(W_5O_{18})_2]\cdot 35H_2O$ (Bruker FRA-106 FT–Raman Spectrometer).

and terminal oxygen atoms ν(W=O_t), while the peak at 893 cm^{-1} was assigned to vibrations ν(Ln–O–W, O–Ln–O, O–W–O) in the central polyhedron {EuO_8} of the heteropoly anion and its associated tungsten atoms from the two lacunary fragments Ln–O–{W_5O_{17}}. Peaks with maxima at 841 and 551 cm^{-1} were attributed to vibrations ν(O–W–O). Peaks observed at lower energies – ranging from 137 to 492 cm^{-1} – were identified as deformation vibrations δ(W=O/O–W–O/Ln–O–W).

3.4 Crystal Structure of Heteropoly compounds with the $[Eu(W_5O_{18})_2]^{9-}$ Anion

Single-crystal X-ray diffraction analysis (XRD) of $Na_9[Eu(W_5O_{18})_2]\cdot 35H_2O$ was performed using an automatic X-ray diffractometer KUMA KM4 (MoKα radiation, λ = 0.71073 Å, graphite monochromator, CCD detector) at 100 K with an Oxford Cryosystem cryostat. Data collection and reduction were carried out using CrysAlis PRO [14].

The structure was solved by direct method using the Olex2 software package [15] with the ShelXT program [16], and structure refinement was performed using the least-squares method with the ShelXL program [17].

The crystal structure and packing of $Na_9[Eu(W_5O_{18})_2]\cdot 35H_2O$ are shown in Figures 3.9–3.11, and the main crystallographic data are presented in Table 3.1. The heteropoly anions in the structure are interconnected through the NaO_6 and NaO_5 polyhedra of the

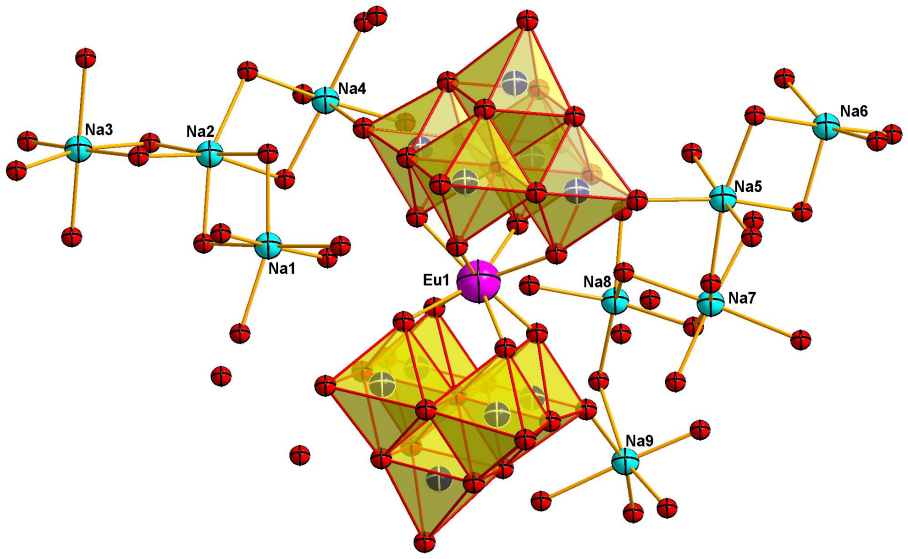

Figure 3.9 Representation of the main structural unit of $Na_9[Eu(W_5O_{18})_2]\cdot 35H_2O$

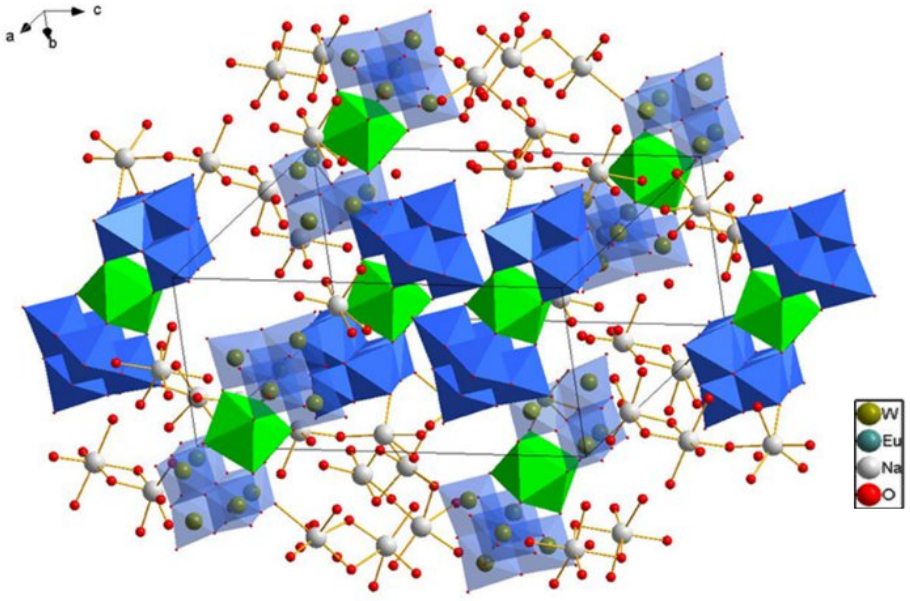

Figure 3.10 Projection of the structure of $Na_9[Eu(W_5O_{18})_2]\cdot 35H_2O$ (cationic sublattice shown as a ball-and-stick model)

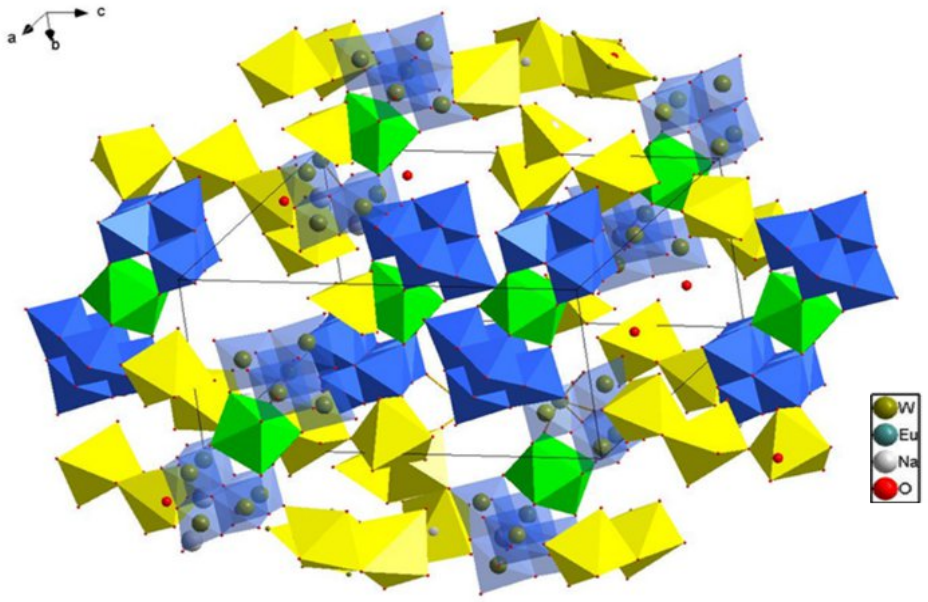

Figure 3.11 Crystal packing of $Na_9[Eu(W_5O_{18})_2]\cdot 35H_2O$ (non-coordinated H_2O molecules shown as red spheres)

Table 3.1 Crystallographic Data for $Na_9[Eu(W_5O_{18})_2]\cdot 35H_2O$

Parameter	Data
Empirical formula	$EuNa_9O_{67}W_{10}4(O)$
Formula weight M_r, a.m.u.	3333.37
Temperature, K	100(2)
Wavelength MoKα, Å	0.71073
Crystal system, space group	Triclinic; *P*–1
Unit cell dimensions (Å)	a = 12.928(4); b = 13.064(4); c = 21.427(6)
α, β, γ (°)	101.04(3). 103.43(3). 103.03(3)
Cell volume V, Å^3	3313.8(18)
Z, d_{calc} (g/cm^3)	2; 3.341
Absorption coefficient μ(MoKα), мм$^{-1}$	18.393
F(000)	2940
Crystal size, mm	0.528 × 0.355 × 0.264
θ range for data collection	2.926° ≤ θ ≤ 36.892°
Index ranges	–21 ≤ *h* ≤ 20 –21 ≤ *k* ≤ 17 –35 ≤ *l* ≤ 35
Reflections collected / unique	30781 / 6955 (R_{int} = 0.0796)
Completeness to θ = 30.00°	99.8 %
Transmission T_{max}/T_{min}	0.086 / 0.013
Refinement method	Full-matrix least-squares on F^2

Table 3.1 (Continuation)

Parameter	Data
Data/parameters	24165 / 724
Goodness-of-fit S on F^2	1.084
Final R indices ($I > 2\sigma_I$)	$R_1 = 0.0829$; $wR^2 = 0.2001$
R indices (all data)	$R_1 = 0.1096$; $wR^2 = 0.2178$
Largest diff. peak/hole $\Delta\rho_{max}/\Delta\rho_{min}$, e/Å^3	6.254 / –7.186

cationic sublattice, which are themselves linked by shared edges or vertices. The $[Eu(W_5O_{18})_2]^{9-}$ heteropoly anion consists of two monolacunary tetradentate fragments $[W_5O_{18}]^{6-}$, derived from the hexatungstate anion with Lindqvist type of structure, which encapsulates the central Eu^{3+} ion, forming a polyhedron $\{EuO_8\}$ in the shape of a square antiprism. The lacunary fragments of $[W_5O_{18}]^{6-}$ coordinated to the Eu(III) heteroatom are rotated relative to each other by an angle of 45º.

3.4.1 Comparison of the Crystal Structure Parameters of $[Eu(W_5O_{18})_2]^{9-}$ Anions in Salts of Different Compositions

To determine the influence of the cationic sublattice composition and the hydration of salts on the structural parameters of the heteropoly anion (Eu–O, W–O, W–O(Eu) bond lengths, O–W–O, O–Eu–O valence angles, and O…O interatomic distances in EuO_8 polyhedra, see Fig. 3.12), a comparison of structural parameters of salts for which deposited CIF files were found [1, 18–19] has been conducted. Data for four single-crystal samples were compared: $Na_9[Eu(W_5O_{18})_2]\cdot 35H_2O$ salts synthesized using different procedures

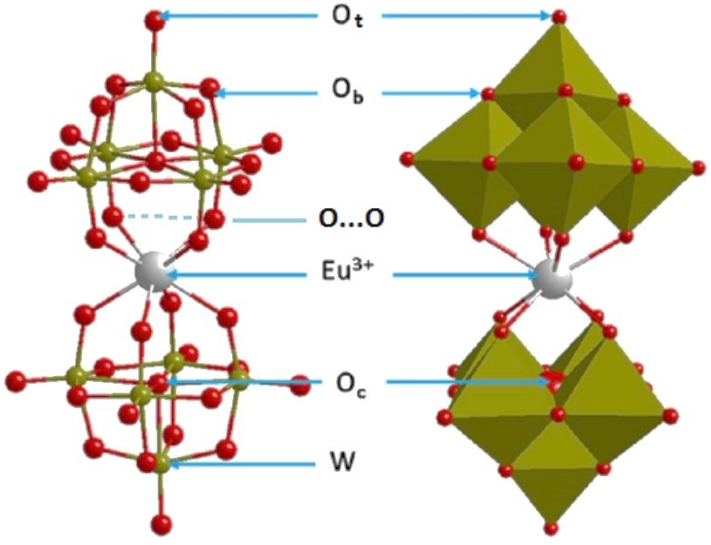

Figure 3.12 Structural fragments of the $[Eu(W_5O_{18})_2]^{9-}$ heteropoly anion used for comparison

Table 3.2 Comparison of bond lengths and valence angles in Eu(III)-containing heteropoly salts

Compound	$Na_9[Eu(W_5O_{18})_2]\cdot 35H_2O$		$Na_9[Eu(W_5O_{18})_2]\times$	$NaSr_4[Eu(W_5O_{18})_2]\times$
Parameter	this research	[18]	$\times 32H_2O$ [1]	$\times 34{,}5H_2O$ [19]
$l_{W=Ot}$	1.75 (1.74–1.75)	1.74 (1.73–1.74)	1.77 (1.77)	1.74 (1.72–1.75)
$l_{W-Ob(eq)}$	1.95 (1.92–1.98)	1.94 (1.92–1.97)	1.95 (1.88–2.00)	1.94 (1.87–2.02)
l_{W-Ob}	2.03 (2.01–2.05)	2.02 (2.00–2.04)	2.02 (1.97–2.04)	2.05 (1.99–2.08)
l_{W-O}	1.91 (1.89–1.93)	1.91 (1.88–1.96)	1.91 (1.88–1.93)	1.90 (1.86–1.95)
l_{W-Ob}	1.78 (1.76–1.81)	1.78 (1.77–1.79)	1.78 (1.73–1.81)	1.79 (1.74–1.83)
l_{W-Oc}	2.32 (2.30–2.34)	2.32 (2.29–2.37)	2.32 (2.27–2.36)	2.31 (2.20–2.42)
$l_{W=Ot(eq)}$	1.74 (1.72–1.76)	1.72 (1.71–1.73)	1.74 (1.70–1.77)	1.71 (1.68–1.75)
$\measuredangle W–O_b–W$	115.7	116.2	116.4	115.6
$\measuredangle W–O_{b(eq)}–W$	114.2	114.7	114.2	114.4
$\measuredangle W–Ocb_{Eu–O}–W$	89.8	89.8	89.8	89.9

(using the procedure developed in this study and isolated in [18] according to the synthesis technique described in [3]), $Na_9[Eu(W_5O_{18})_2]\cdot 32H_2O$ salt with a different hydration composition and fewer non-coordinated H_2O molecules in the structural cavities, and $NaSr_4[Eu(W_5O_{18})_2]\cdot 34.5H_2O$ salt with a different cationic component and different nature of the attachment of double-charged strontium cations to the heteropoly anion.

Analysis of the structural parameters of compounds with Eu(III) heteroatom (Table 3.2) shows that changes in the composition of the cationic sublattice (single- or double-charged cations of s-metals) or the presence of varying amounts of non-coordinated H_2O molecules in the structural cavities do not significantly affect the bond lengths and valence angles in the $[Eu(W_5O_{18})_2]^{9-}$ heteropoly anion.

Based on the single-crystal X-ray diffraction analysis results, it has been shown that changes in the composition of the cationic sublattice (the presence of SrO_8 polyhedra, which include both terminal and bridging oxygen atoms from the $[W_5O_{18}]^{6-}$ anion, as well as isolated $[Sr(H_2O)_8]^{2+}$ cations) and the presence of varying numbers of H_2O molecules in the structure (32 or 35 molecules per one formula unit) do not affect the bond lengths and valence angles in the $[Eu(W_5O_{18})_2]^{9-}$ heteropoly anion in crystalline salts.

3.5 Summary

The conditions for the synthesis of the crystalline sodium salt of heteropoly decatungstoeuropate(III), $Na_9[Eu(W_5O_{18})_2]\cdot 35H_2O$, with a plate-like surface micromorphology have been developed. For a rational synthesis, it is necessary to use an aqueous solution of the system $Eu(NO_3)_3 – Na_2WO_4 – HNO_3 – H_2O$, acidified with nitric acid to Z = 0.80, with a ratio of ν(Eu) : ν(W) = 1 : 10, and salting out by the adding of propan-2-one. Infrared and Raman spectroscopy methods established a set of vibrations characteristic for the hetero-

poly decatungstoeuropate(III) anion with the Peacock–Weakley type of structure, $[Eu(W_5O_{18})_2]^{9-}$.

This study presents the results of determining the crystal structure of Eu(III)-containing heteropoly tungstate. From the perspective of experimental chemistry, the novelty of the study lies in establishing the synthesis conditions (a new procedure) and the crystal structure of the normal salt $Na_9[Eu(W_5O_{18})_2]\cdot 35H_2O$, characterizing its structure and spectral properties. From the perspective of theoretical chemistry, the novelty and practical significance of the work lies in the determination of the structure of a "pure inorganic" heteropoly compound and determining the structural parameters based on bond lengths and valence angles in the WO_6, EuO_8, NaO_6, and NaO_5 polyhedra, which serve as fundamental reference data and may be used as a reliable source of information. The uniqueness of the result also lies in demonstrating the independence of the influence of the cationic sublattice composition and the number of non-coordinated H_2O molecules on the structural parameters (bond lengths and valence angles) in the heteropoly anion $[Eu(W_5O_{18})_2]^{9-}$ with the Peacock–Weakley type of structure.

Acknowledgments

The study was carried out within the framework of a fundamental project "Compounds of *d*- and *f*-metals with polyoxometalate anions and prediction of interaction in complex oxide systems" (grant provider – Ministry of Education and Science of Ukraine, grant ID 0122U000762).

Keywords

- Polyoxometalate
- heteropoly anion
- Europium
- Peacock–Weakley type anion
- crystal structure

References

1. *Sugeta M., Yamase T.* Crystal Structure and Luminescence Site of $Na_9[Eu(W_5O_{18})_2]\cdot 32H_2O$ // Bull. Chem. Soc. Jpn. 1993. Vol. 66, No. 2. P. 444–449. DOI: https://doi.org/10.1246/bcsj.66.444.
2. *Zhang T. R., Lu R., Zhang H. Y., Xue P. Ch., Feng W., Liu X. L., Zhao B., Zhao Y. Y., Lia T. J., Yao J. N.* Highly ordered photoluminescent self-assembled films based on polyoxotungstoeuropate complex $Na_9[EuW_{10}O_{36}]$ // J. Mater. Chem. 2003. Vol. 13, No. 3. P. 580–584. DOI: https://doi.org/10.1039/B210965D.
3. *Peacock R.D., Weakley T.J.R.* Heteropoly tungstate complexes of the lanthanide elements. Part I. Preparation and reactions // J. Chem. Soc. A Inorg. Phys. Theor. 1971. P. 1836–1839. DOI: http://dx.doi.org/10.1039/J19710001836.

4. *Lu J., Kang Q., Xiao J., Wang T., Fang M., Yu L.* Luminescent, stabilized and environmentally friendly $[EuW_{10}O_{36}]^{9-}$–T Chitosan films for sensitive detection of hydrogen peroxide // Carbohydrate Polymers. 2018. Vol. 200. P. 560–566. DOI: https://doi.org/10.1016/j.carbpol.2018.08.038.
5. *Liu S.-M., Zhang Zh., Li X.-H., Jia H.-J., Liu S.-X.* Synthesis and photophysical properties of crystalline $[EuW_{10}O_{36}]^{9-}$-based polyoxometalates with lanthanide ions as counter cations // J. Alloys Compd. 2018. Vol. 761. P. 52–57. DOI: https://doi.org/10.1016/j.jallcom.2018.05.144.
6. *Wang Z., Zhang R., Ma Y., Peng A., Fua H., Yao J.* Chemically responsive luminescent switching in transparent flexible self-supporting $[EuW_{10}O_{36}]^{9-}$ agarose nanocomposite thin films // J. Mater. Chem. 2010. Vol. 20, No. 2. P. 271–277. DOI: https://doi.org/10.1039/B917739F.
7. *Zhang H., Li X., Zhang L., Zhou Y., Ren X., Liu M.* Color-tunable and white-light emitting thin films based on pure inorganic polyoxometalates $Na_9Eu_mTb_nCe_{1-m-n}W_{10}O_{36}$ // J. Alloys Compounds. 2018. Vol. 749. P. 229–235. DOI: https://doi.org/10.1016/j.jallcom.2018.03.277.
8. *Zhang H., Guo L., Xie Z., et al.* Tunable Aggregation-Induced Emission of Polyoxometalates via Amino Acid-Directed Self-Assembly and Their Application in Detecting Dopamine // Langmuir. 2016. Vol. 32, No. 51. P. 13736−13745. DOI: https://doi.org/10.1021/acs.langmuir.6b03709.
9. *Mariichak O.Yu., Ivantsova E.S., Rozantsev G.M., Radio S.V.* Thulium–containing heteropoly tungstate with Peacock–Weakley anion: Synthesis, properties, and surface micromorphology // Voprosy Khimii i Khimicheskoi Tekhnologii. 2015. No. 3. P. 38–44. URI: https://udhtu.edu.ua/public/userfiles//file/VHHT/2015/3/Mariichak.pdf.
10. *Mariichak O.Yu., Ignatyeva V.V., Baumer V.N., Rozantsev G.M., Radio S.V.* Heteropoly decatungstolanthanidates(III) with Peacock–Weakley type anion: Synthesis and crystal structure of isostructural salts $Na_9[Ln(W_5O_{18})_2]\cdot 35H_2O$ (Ln=Gd, Er) // J. Chem. Crystallogr. 2020. Vol. 50, No. 3. P. 255–266. DOI: https://doi.org/10.1007/s10870-020-00845-2.
11. *Mariichak O.Y., Kaabel S., Karpichev Y.A., Rozantsev G.M., Radio S.V., Pichon C., Bolvin H., Sutter J.-P.* Crystal Structure and Magnetic Properties of Peacock–Weakley Type Polyoxometalates $Na_9[Ln(W_5O_{18})_2]$ (Ln = Tm, Yb): Rare Example of Tm(III) SMM // Magnetochemistry. 2020. Vol. 6, No. 4. Art. 53. DOI: https://doi.org/10.3390/magnetochemistry6040053.
12. *Shiozaki R., Inagaki A., Nishino A., Nishio E., Maekawa M., Kominami H., Kera Y.* Spectroscopic investigation of a series of sodium lanthanide decatungstates, $Na_7H_2Ln(III)(W_5O_{18})_2\cdot nH_2O$ (Ln: La–Yb): the contribution of $4f^n$ electrons to bonding interaction among Ln(III) and polyoxotungstates // J. Alloys Compd. 1996. Vol. 234, No. 2. P. 193–198. DOI: https://doi.org/10.1016/0925-8388(95)02112-4.
13. *Subintoro P.J., Carter K.P.* Structural and vibrational properties of lanthanide Lindqvist polyoxometalate complexes // Dalton Trans. 2024. Vol. 53, No. 22. P. 9526–9539. DOI: https://doi.org/10.1039/D4DT00786G.
14. Rigaku Oxford Diffraction. CrysAlis PRO. Rigaku Oxford Diffraction, Yarnton, England. 2015. URI: https://rigaku.com/products/crystallography/x-ray-diffraction/crysalispro.
15. *Dolomanov O.V., Bourhis L.J., Gildea R.J., Howard J.A.K, Puschmann H.* OLEX2: A complete structure solution, refinement and analysis program // J. Appl Cryst. 2009. Vol. 42. P. 339–341. DOI: https://doi.org/10.1107/S0021889808042726.
16. *Sheldrick G.M.* SHELXT – Integrated space-group and crystal-structure determination // Acta Cryst. 2015. Vol. A71, Pt. 1. P. 3–8. https://doi.org/10.1107/S2053273314026370.
17. *Sheldrick G.M.* Crystal structure refinement with SHELXL // Acta Cryst. 2015. Vol. C71, Pt. 1. P. 3–8. DOI: https://doi.org/10.1107/S2053229614024218.
18. *Yan Y., Li B., Li W., Li H., Wu L.* Controllable vesicular structure and reversal of a surfactant-encapsulated polyoxometalate complex // Soft Matter. 2009. Vol. 5, No. 20. P. 4047–4053. DOI: https://doi.org/10.1039/B912011D.
19. *Yamase T., Ozeki T., Ueda K.* Structure of $NaSr_4[EuW_{10}O_{36}]\cdot 34.5H_2O$. Acta Cryst. 1993. Vol. C49. P. 1572–1574. DOI: https://doi.org/10.1107/S0108270193002082.